Impairment of CCR6+ and CXCR3+ th cell migration in HIV-1 infection is rescued by modulating actin polymerization

Cecchinato, Valentina ; Bernasconi, Enos ; Speck, Roberto F ; Proietti, Michele ; Sauermann, Ulrike ; D'Agostino, Gianluca ; Danelon, Gabriela ; Rezzonico Jost, Tanja ; Grassi, Fabio ; Raeli, Lorenzo ; Schöni-Affolter, Franziska ; Stahl-Hennig, Christiane ; Uguccioni, Mariagrazia ; Swiss HIV Cohort Study

Abstract: CD4(+) T cell repopulation of the gut is rarely achieved in HIV-1-infected individuals who are receiving clinically effective antiretroviral therapy. Alterations in the integrity of the mucosal barrier have been indicated as a cause for chronic immune activation and disease progression. In this study, we present evidence that persistent immune activation causes impairment of lymphocytes to respond to chemotactic stimuli, thus preventing their trafficking from the blood stream to peripheral organs. CCR6(+) and CXCR3(+) Th cells accumulate in the blood of aviremic HIV-1-infected patients on long-term antiretroviral therapy, and their frequency in the circulation positively correlates to levels of soluble CD14 in plasma, a marker of chronic immune activation. Th cells show an impaired response to chemotactic stimuli both in humans and in the pathogenic model of SIV infection, and this defect is due to hyperactivation of cofilin and inefficient actin polymerization. Taking advantage of a murine model of chronic immune activation, we demonstrate that cytoskeleton remodeling, induced by okadaic acid, restores lymphocyte migration in response to chemokines, both in vitro and in vivo. This study calls for novel pharmacological approaches in those pathological conditions characterized by persistent immune activation and loss of trafficking of T cell subsets to niches that sustain their maturation and activities.

DOI: https://doi.org/10.4049/jimmunol.1600568

The Journal of Immunology

Impairment of CCR6$^+$ and CXCR3$^+$ Th Cell Migration in HIV-1 Infection Is Rescued by Modulating Actin Polymerization

Valentina Cecchinato, Enos Bernasconi, Roberto F. Speck, Michele Proietti, Ulrike Sauermann, Gianluca D'Agostino, Gabriela Danelon, Tanja Rezzonico Jost, Fabio Grassi, Lorenzo Raeli, Franziska Schöni-Affolter, Christiane Stahl-Hennig, Mariagrazia Uguccioni and the Swiss HIV Cohort Study

J Immunol 2017; 198:184-195; Prepublished online 28 November 2016;
doi: 10.4049/jimmunol.1600568
http://www.jimmunol.org/content/198/1/184

The Journal of Immunology is published twice each month by
The American Association of Immunologists, Inc.,
9650 Rockville Pike, Bethesda, MD 20814-3994.

Print ISSN: 0022-1767 Online ISSN: 1550-6606.

Impairment of CCR6$^+$ and CXCR3$^+$ Th Cell Migration in HIV-1 Infection Is Rescued by Modulating Actin Polymerization

Valentina Cecchinato,* Enos Bernasconi,† Roberto F. Speck,‡ Michele Proietti,* Ulrike Sauermann,§ Gianluca D'Agostino,* Gabriela Danelon,* Tanja Rezzonico Jost,* Fabio Grassi,*,¶ Lorenzo Raeli,* Franziska Schöni-Affolter,‖ Christiane Stahl-Hennig,§ Mariagrazia Uguccioni,*,# and the Swiss HIV Cohort Study[1]

CD4$^+$ T cell repopulation of the gut is rarely achieved in HIV-1–infected individuals who are receiving clinically effective antiretroviral therapy. Alterations in the integrity of the mucosal barrier have been indicated as a cause for chronic immune activation and disease progression. In this study, we present evidence that persistent immune activation causes impairment of lymphocytes to respond to chemotactic stimuli, thus preventing their trafficking from the blood stream to peripheral organs. CCR6$^+$ and CXCR3$^+$ Th cells accumulate in the blood of aviremic HIV-1–infected patients on long-term antiretroviral therapy, and their frequency in the circulation positively correlates to levels of soluble CD14 in plasma, a marker of chronic immune activation. Th cells show an impaired response to chemotactic stimuli both in humans and in the pathogenic model of SIV infection, and this defect is due to hyperactivation of cofilin and inefficient actin polymerization. Taking advantage of a murine model of chronic immune activation, we demonstrate that cytoskeleton remodeling, induced by okadaic acid, restores lymphocyte migration in response to chemokines, both in vitro and in vivo. This study calls for novel pharmacological approaches in those pathological conditions characterized by persistent immune activation and loss of trafficking of T cell subsets to niches that sustain their maturation and activities. ***The Journal of Immunology*****, 2017, 198: 184–195.**

Infection with HIV-1 in humans is characterized by a severe depletion of memory CD4$^+$ T cells, both in the blood and in the mucosal compartment (1), and by impaired immune responses to many pathogens (2). CD4$^+$ T cell reduction during infection has been associated not only with direct viral cytotoxicity (3), but with a more generalized state of chronic immune activation, which contributes to cell loss and to immune dysfunction, ultimately leading to disease progression (4, 5). This hypothesis is corroborated by many studies indicating that: 1) during infection the markers of immune activation are increased, and they correlate with a poor prognosis (6–9); 2) proinflammatory cytokines and chemokines are expressed at high levels in the lymphoid organs of SIV-infected macaques and of HIV-1–infected patients (10–12); 3) prolonged immune activation in mice models results in T cell immunodeficiency (13) and in lymphoid architecture disruption (14); and 4) natural hosts of SIV, which despite the high viral load do not progress to AIDS, have a much lower immune activation than that found in pathogenic models of SIV infection (15).

A possible cause of chronic systemic immune activation is the translocation of microbial products from the gastrointestinal mucosa to the circulation, due to virologic and immunologic events (16–19). Indeed, plasma levels of LPS are increased in chronically HIV-1–infected patients and SIV-infected macaques and correlate with markers of immune activation, such as the frequency of circulating CD38$^+$HLA-DR$^+$CD8$^+$ T cells or plasma levels of soluble CD14 (sCD14) (16). An important role in the maintenance of the integrity of the mucosal barrier has been attributed to Th17 cells (20), a subset of Th cells that are depleted in HIV-1 (21), and in

*Institute for Research in Biomedicine, University of Italian Switzerland, 6500 Bellinzona, Switzerland; †Division of Infectious Diseases, Regional Hospital, 6903 Lugano, Switzerland; ‡Division of Infectious Diseases and Hospital Epidemiology, University Hospital of Zurich, University of Zurich, 8091 Zurich, Switzerland; §Unit of Infection Models, German Primate Center, 37077 Göttingen, Germany; ¶Department of Medical Biotechnology and Translational Medicine, University of Milan, 20133 Milan, Italy; ‖Swiss HIV Cohort Study Data Center, University Hospital, 1011 Lausanne, Switzerland; and #Department of Biomedical Sciences, Humanitas University, 20089 Milan, Italy

[1]All authors in the Swiss HIV Cohort Study appear at the end of this article.

ORCID: 0000-0001-6229-046X (U.S.).

Received for publication March 31, 2016. Accepted for publication October 24, 2016.

This work was supported within the framework of the Swiss HIV Cohort Study (Study 719), funded by Swiss National Science Foundation Grant 134277. V.C. has received European Union Marie Curie Fellowship FP7-IEF-235200 (Migration and Differentiation of Th17 Cells in HIV/SIV Infection) for the work performed in the laboratory of M.U. M.U. has received funding for this project from the European Union's programs for research, technological development, and demonstration under agreements INNOCHEM, Grant LSHB-CT-2005-518167 (6th Framework Program); DEC-VAC, Grant LSHP-CT-2005-018685 (6th Framework Program); ADITEC, Grant 280873 (7th Framework Program); and TIMER, Grant 281608 (7th Framework Program). This project was further supported by Swiss National Science Foundation Grant 3100A0-143718/1 (to M.U.), the San Salvatore Foundation, the Novartis Foundation (to M.U.), the Gottfried and Julia Bangerter-Rhyner Foundation, the Helmut Horten Foundation, and the Institute for Arthritis Research.

Address correspondence and reprint requests to Prof. Mariagrazia Uguccioni and Dr. Valentina Cecchinato, Institute for Research in Biomedicine, Via Vela 6, 6500 Bellinzona, Switzerland. E-mail addresses: mariagrazia.uguccioni@irb.usi.ch (M.U.) and valentina.cecchinato@irb.usi.ch (V.C.)

The online version of this article contains supplemental material.

Abbreviations used in this article: ART, antiretroviral therapy; HD, healthy donor; MFI, mean fluorescence intensity; mo-DC, monocyte-derived dendritic cell; OA, okadaic acid; PP, Peyer's patch; rMFI, relative mean fluorescence intensity; sCD14, soluble CD14; SHCS, Swiss HIV Cohort Study.

pathogenic SIV infection (22, 23). In contrast, nonpathogenic models of SIV infection as well as elite controller patients maintain normal frequencies of Th17 cells (21, 24, 25).

Although long-term antiretroviral therapy (ART) is able to restore Th17 cells in the bloodstream, only a partial reconstitution is achieved in the mucosal compartment (26–28). The mechanisms leading to a preferential depletion of Th17 cells have been partially elucidated: several studies have shown that Th17 cells are more permissive than Th1 cells to HIV-1 infection both in vitro and in vivo (29–32). Although Th1 cells, which express the chemokine receptors CXCR3, CCR5, and CXCR4, have been shown to be relatively resistant to HIV infection in vitro (29), the predominant susceptibility of Th17 cells to some HIV strains has been linked to the expression of the chemokine receptors CCR6, CCR9, CCR5, and of the integrin $\alpha_4\beta_7$, which are also essential for their homing to the intestinal mucosa (33–35). In the SIV infection model it has been demonstrated that, despite effective ART, intestinal Th17 cell function is severely impaired (36), suggesting that during prolonged viral suppression, the incomplete gut reconstitution of this subpopulation accounts for the maintenance of persistent chronic immune activation.

Leukocyte migration to tissues is controlled by the local expression of chemokines, which trigger an intracellular cascade of events resulting in cytoskeleton reorganization (37). In particular, F-actin generation results in a change of cell shape, which is essential for effective migration, and depends on many cellular factors involved in the remodeling of F-actin stores. Among these, cofilin is an actin-severing protein that, in its active nonphosphorylated form, binds to the end of F-actin and cleaves the filaments into shorter fragments. On one side this process reduces intracellular F-actin stores, but on the other side it also introduces new substrates for further actin polymerization (38). Phosphorylation on Ser^3 by LIM kinase-1 leads to cofilin inactivation and inhibits the ability of this protein to depolymerize F-actin (39, 40).

In this study, we have elucidated mechanisms that might be responsible for a poor repopulation of Th cells in the gut of HIV-1–infected patients, despite successful treatment with ART. We found that $CCR6^+$ and $CXCR3^+$ Th cells accumulate in the blood of treated patients, their frequency in the circulation correlates with chronic immune activation, and that $CCR6^+$ cells are depleted in the colonic lamina propria of SIV-infected macaques. In HIV-1–infected patients regardless of therapy and in SIV-infected macaques, migration of Th cells in response to chemotactic stimuli is impaired and is associated with perturbation of actin polymerization. Using an in vivo model (14), we demonstrate that chronic immune activation per se is sufficient to dampen Th cell migration, which can be restored by pharmacological modulation of cytoskeleton activity.

Materials and Methods

Ethics statement

Colony-bred rhesus monkeys of Indian origin were housed at the German Primate Center under standard conditions according to the German Animal Welfare Act, which complies with the European Union guidelines on the use of nonhuman primates for biomedical research. Animals belonged to studies approved by the Ethics Committee authorized by the Lower Saxony State Office for Consumer Protection with the project licenses 33.14-4502-04-017/07, 33.14.42502-04-072/08, and 33.14-42502-04-10/0037. According to section 11 of the German Animal Welfare Act, the German Primate Center is permitted to breed and house nonhuman primates under license no. 392001/7 issued by the local veterinary authorities. Measures of animal welfare and reduction of suffering comprise a 12:12 h light/dark schedule, provision of dry monkey biscuits supplemented with fresh fruit or vegetables twice daily, and fresh water access ad libitum. Additionally, for environmental enrichment, animals were offered feeding puzzles, varying toys, and wood sticks for gnawing. Monkeys were kept under permanent health care supervision by trained staff and veterinarians. Moreover, supervision and advice were provided by the institutional welfare officer as demanded by the German Animal Welfare Act. SIV-infected rhesus macaques were caged in groups of two or three animals, permitting social behavior. In case of suffering predefined by a scoring system on termination criteria, monkeys were humanely killed in deep anesthesia by an overdose of pentobarbital given i.v.

C57BL/6 mice were maintained in the specific pathogen-free animal facility of the Institute for Research in Biomedicine. All animal experiments were performed in accordance with the Swiss Federal Law (Animal Welfare Act RS 455, Tierschutzgesetz, https://www.admin.ch/opc/de/classified-compilation/20022103/index.html) and the Cantonal rules on experiments with animals (Regolamento Cantonale sulla Protezione degli Animali). The experiments were evaluated by the Cantonal animal experimentation committee (Comitato Etico Cantonale del Ticino, Switzerland) and approved under authorization no. TI17/2010.

HIV-1–infected patients were recruited from the Swiss HIV Cohort Study (SHCS). The SHCS was approved by the local ethical committees of the participating centers (Kantonale Ethikkommission Zürich [KEK-ZH-NR: EK-793]; Comitato Etico Cantonale, Repubblica e Cantone Ticino [CE 813]), and written informed consent was obtained from all participants.

Animals

For this study 63 adult colony-bred rhesus monkeys of Indian origin comprising 17 naive and 46 experimentally infected with SIV_{mac239} or SIV_{mac251} between 4 and 12 y old were used. Animals had been infected by the i.v., intrarectal, or tonsillar route with SIV_{mac251} or SIV_{mac239}, and blood was collected either in the early postacute phase (weeks 5–6 postinfection, $n = 6$) or in the late-chronic phase of infection (>13 wk postinfection, $n = 40$). Intestinal biopsies were collected longitudinally from six animals before infection (preinfection), 10 d postinfection, and 13 wk postinfection, as described before (41). To obtain blood samples animals were sedated intramuscularly with 10 mg of ketamine per kilogram body weight. For deeper anesthesia required for the collection of intestinal biopsies or as premedication for euthanasia, a mixture of ketamine, xylazine, and atropine was injected i.m.

A total of 110 C57BL/6 mice were purchased from Harlan Laboratories (Udine, Italy). Age- and sex-matched mice (6–8 wk old) were randomly assigned to two groups that were injected i.p. for 7 d either with PBS (control, $n = 50$) or with 0.1 mg/kg/d R848 ($n = 50$). Air pouches were established in R848-treated and in controls animals by injecting s.c. 5 and 3 ml of air at day 0 and day 3, respectively. At day 6, mice were injected in the air pouch with 1000 pmol CXCL12, 1000 pmol okadaic acid (OA), or with a combination of 1000 pmol CXCL12 and 1000 pmol OA. PBS (200 μl) was injected to determine basal cell recruitment. After 6 h, cells were collected from the air pouch and analyzed by flow cytometry. To calculate the total cell number in Peyer's patches (PP), all the PP from the entire intestine were collected from R848-treated and control mice. Cells were recovered after mechanical destruction and counted to obtain the total number of cells in PP per intestine (cells per intestine). Cells were then stained with the indicated Abs to determine the frequency of different subpopulations and analyzed by flow cytometry. Spleens from 10 untreated C57BL/6 mice (6–8 wk old) were collected to obtain cells for in vitro experiments to assess the influence of R848 on cell proliferation, apoptosis, and migration.

Patients

We enrolled 58 HIV-1–infected patients who were followed in the SHCS (http://www.shcs.ch) (42). Patients were divided into three groups according to their CD4 nadir count and the use of ART in the last 3 y. Group A comprised 15 ART-naive patients. Group B included 29 patients on ART for >3 y and with a CD4 nadir of <100 cells/μl of blood. Group C included 14 patients on ART for >3 y and with a CD4 nadir of >350 cells/μl of blood. Exclusion criteria included opportunistic infections, acute somatic diseases, neoplastic diseases, immune-suppressive therapies, and chronic hepatitis B virus or hepatitis C virus coinfection. Features of all patients are shown in Table I.

Cell isolation

PBMCs were isolated from peripheral blood of both human and macaque specimens using Ficoll-Hypaque density centrifugation within 24 h from blood withdrawal. PBMCs from healthy donors (HD) were isolated from buffy coats (Central Laboratory of the Swiss Red Cross, Basel, Switzerland), whereas blood from HIV-1–infected patients was collected in BD Vacutainer CPT cell preparation tubes containing sodium citrate as anticoagulant (362782; BD Biosciences). Total $CCR6^+$ and $CXCR3^+$ cells, which includes

B and T lymphocytes, were isolated from PBMCs by a first incubation with anti–CCR6-PE (11A9; BD Pharmingen) or anti–CXCR3-PE (1C6; BD Pharmingen), followed by PE magnetic beads sorting (Miltenyi Biotec).

For the experiments performed with cells from HD exposed to plasma from HIV-1–infected patients, CD4$^+$ cells were enriched using CD4 magnetic beads (Miltenyi Biotec), and CCR6$^+$CD45RA$^-$ cells were sorted using BD FACSAria III (BD Biosciences).

Monocytes were isolated from PBMCs using CD14 magnetic beads (Miltenyi Biotec), and monocyte-derived dendritic cells (mo-DCs) were generated as previously described (43). Briefly, CD14$^+$ cells were cultured for 4 d in RPMI 1640 medium supplemented with 10% FCS, 1000 U/ml IL-4, and 50 ng/ml GM-CSF. Cells were then stimulated overnight either with LPS (2 μg/ml) or with *Candida albicans* (at the ratio of 3:1) and the supernatants were collected to evaluate CCL20 and CXCL10 production by stimulated mo-DCs.

Murine splenocytes were isolated after mechanical destruction of the spleen, followed by red blood cell lysis according to standard protocols. CD4$^+$ T cells were isolated from splenocytes using CD4 magnetic beads (LT34; Miltenyi Biotec). For experiments in which splenocytes were cultured in the presence of R848, enriched CD4$^+$ splenocytes were sorted using a BD FACSAria III (BD Biosciences) as naive CCR6$^-$ (CD4$^+$CD25$^-$CD62L$^+$CD44$^-$CCR6$^-$), memory CCR6$^-$ (CD4$^+$CD25$^-$CD44$^+$CCR6$^-$), or memory CCR6$^+$ (CD4$^+$CD25$^-$CD44$^+$CCR6$^+$) CD4$^+$ cells.

Flow cytometric analysis

For surface staining of human and macaque specimens, cell suspensions were incubated with the appropriate combination of the following mAbs: CD3-allophycocyanin-Cy7 (SP34-2; BD Pharmingen), CD4-PerCP-Cy5.5 (L200; BD Pharmingen), CD20-FITC (2H7; AbD Serotec), CD45RA-FITC (ALB11; Beckman Coulter), CCR6-PE (11A9; BD Pharmingen), CCR7-PE-Cy7 (3D12; BD Pharmingen), CXCR3–Alexa Fluor 488 (1C6; BD Pharmingen), CXCR3-PE (1C6; BD Pharmingen).

For intracellular staining, cells were fixed for 30 min with cold paraformaldehyde (4%) in PBS and permeabilized for 2 min with 0.1% Triton X-100. Staining was then performed using rabbit mAbs specific for cofilin (D3F9; Cell Signaling Technology), or phospho-cofilin (Ser^3) (77G2; Cell Signaling Technology), followed by anti-rabbit IgG–Alexa Fluor 633 (A-2107; Life Technologies).

Surface staining of murine specimens was performed using a combination of the following mAbs: CD3-PE (145-2C11; BioLegend), CD3–Alexa Fluor 647 (17A2; BioLegend), CD4-FITC (GK1.5; BioLegend), CD4-PerCP (GK1.5; BioLegend), CD25-PE-Cy7 (PC61; BioLegend), CD44-FITC (IM7; BioLegend), CD45R/B220–Pacific Blue (RA3-6B2; BioLegend), CD45R/B220-PerCP-Cy5.5 (RA3-6B2; eBioscience), CD62L-allophycocyanin (MEL-14; eBioscience), F4/80-allophycocyanin-Cy7 (BM8; BioLegend), Gr1-biotin (RB6-8C5; BD Pharmingen), CD11b-PE-Cy7 (M1/70; BioLegend), CXCR4-PE (L276F12; BioLegend), CXCR3–Brilliant Violet 421 (CXCR3-173; BioLegend), CCR6-PE (29-2L17; BioLegend).

The samples were acquired with BD LSRFortessa (BD Biosciences), and the results were analyzed with FlowJo software (Tree Star). Relative mean fluorescence intensity (rMFI) was calculated as the ratio between stained and unstained samples; gating strategy is provided in Supplemental Fig. 1A.

Immunohistochemistry

Formalin-fixed paraffin-embedded tissues were cut into 5-μm slices and used for immunohistochemistry. Ag retrieval was performed with Dako target retrieval solution (pH 6, S1699) according to the manufacturer's instructions, and the slides were incubated with the appropriate primary Ab for 2 h at room temperature. For Ag detection the following primary Abs were used: rabbit anti-human CD3 (1 μg/ml, A0452; Dako), mouse anti-human CXCL10 (1 μg/ml, 33036; R&D Systems), mouse anti-human CCR6 (0.5 μg/ml, 53103; R&D Systems), mouse anti-human CXCR3 (0.5 μg/ml, 49801; R&D Systems), rabbit-anti human CCL20 (0.5 μg/ml, ab9829; Abcam), mouse anti-human CD4 (1:100 dilution, 1F6; AbD Serotec), and rat anti-mouse CCR6 (2.5 μg/ml, 18B9E6; Novus Biologicals). Detection of positive cells was achieved using a MACH 4 universal HRP polymer detection kit mouse/rabbit (M4U534H) or rat-on-mouse HRP polymer (RT517G) from Biocare Medical, according to the manufacturer's instructions. Images were acquired using a ×40/0.95 numerical aperture Plan Apo objective on a Nikon Eclipse E800 upright microscope, equipped with the digital camera DXM1200 (Nikon), and using Act-1 software version 2.7 (Nikon). Quantitative analysis was performed with a custom-made macro, using the open-source image analysis software Fiji (44). Images were composed in Photoshop CS5 (Adobe).

Quantitative real-time PCR and plasma viral load in macaques

RNA extraction was performed using standard protocols, after isolation and resuspension in TRIzol reagent (15596; Invitrogen). Retrotranscription was performed using Moloney murine leukemia virus reverse transcriptase (28025; Invitrogen) at 500 ng of RNA per sample and 250 ng of random primers, according to the manufacturer's instructions. TaqMan gene expression assays from Applied Biosystems were used to detect specific transcript levels (protocol as suggested by the manufacturer): *CFL1* Hs02621564_g1, *18S* rRNA 4352930E. The following set of primers/probe was used to detect *HIV1-NEF*: 5′-GCACGGCAAGAGGCGA-3′ (forward primer), 5′-GAGGTGGGTTGCTTTGATAGAG-3′ (reverse primer), 5′-CGGCGACTGGA AGAAGCGGAGA-3′ (FAM Probe) as previously described (45). The 7900HT fast real-time PCR system (Applied Biosystems) was used to perform the detection. Data were normalized on the specific 18S rRNA values and expressed as arbitrary units.

Viral RNA copies were quantified in purified SIV RNA from plasma using TaqMan-based real-time PCR on an ABI Prism 7500 sequence detection system (Applied Biosystems) as described (46).

Chemokine and sCD14 detection

The concentration of CCL20 in the supernatant of human mo-DCs was determined using a sandwich ELISA kit (DM3A00; R&D Systems), according to the manufacturer's protocol. CXCL10 levels in the supernatant of human mo-DCs were determined using the BD cytometric bead array human IP-10 flex set (558280; BD Biosciences), according to the manufacturer's instructions. The concentration of human sCD14 in the plasma of HD and HIV-1–infected patients was determined using a sandwich ELISA kit (DC140; R&D Systems), according to the manufacturer's protocol.

Chemotaxis assay

HTS Transwell-96 permeable support with 3.0-μm pore polycarbonate membrane (3386; Corning) were used to assess migration of CCR6$^+$ or CXCR3$^+$ cells isolated from human or macaque PBMCs or of murine CD4$^+$ splenocytes isolated from C57BL/6 mice. Briefly, after an overnight culture, 15×10^4 cells were diluted in chemotaxis buffer (RPMI 1640 supplemented with 0.05% pasteurized human albumin) and added to the upper wells. For assessing chemotaxis of human or macaque cells, recombinant human CCL20 or CXCL10 (R&D Systems) was diluted in chemotaxis buffer and added to the bottom wells. For assessing chemotaxis of murine cells, recombinant mouse CCL20 or CXCL12 (R&D Systems) was diluted in chemotaxis buffer and added to the bottom wells. For cofilin inhibition assays, 250 nM OA was added to the chemokine in the bottom wells. Migration was allowed to proceed for 90 min at 37°C in 5% CO_2. Migrated cells were collected from the bottom well, stained with CD3-allophycocyanin-CY7, CD4-PercP-Cy5.5, and CD20-FITC, suspended in a fixed volume, and counted at constant speed with a BD LSRFortessa. Chemotaxis index was calculated as the fold increase in the number of migrated cells in response to chemokine over the spontaneous cell migration in response to chemotaxis buffer alone.

Cell tracking

CD4$^+$CCR6$^+$CD45RA$^-$ sorted T cells were stained with 5 μM CFSE, using the CellTrace CFSE cell proliferation kit (C34554; Invitrogen Molecular Probes) according to the manufacturer's instructions. Ninety-six–well flat-bottom plates were precoated with 10 μg/ml fibronectin, and a total of 1×10^4 cells/well were seeded in 100 μl of RPMI 1640 medium supplemented with 5% human plasma from HD or a pool of plasma from five HIV-1–infected patients under long-term ART. After 1 h at 37°C in 5% CO_2, cell random movements were recorded for 3 h, using the BD Pathway 855 imager, acquiring a picture every 2 min for both transmitted light and green fluorescence for CFSE, to check the viability and perform cell tracking, with an Olympus Plan N ×10, numerical aperture of 0.30 objective. Track mean speed (micrometers per minute) was obtained by tracing the spots in the fluorescence channel using Bitplane Imaris 8.0.

Actin polymerization assay

F-actin content was determined with FITC-coupled phalloidin (P5282; Sigma-Aldrich) in human CCR6$^+$ or CXCR3$^+$ cells following chemokine receptor triggering as previously described (47). Briefly, stimulations were performed with 100 nM CCL20 or 100 nM CXCL10, respectively. The reaction was stopped after 15 s and cells were fixed for 30 min with cold paraformaldehyde (4%) in PBS. After fixation, cells were permeabilized with 0.1% Triton X-100, stained with 4 μg/ml FITC-conjugated phalloidin, and analyzed by flow cytometry. For cofilin inhibition assays, cells were preincubated for 15 min at 37°C in the absence or presence of 250 nM OA. All stimulations were performed in duplicate. F-actin content is indicated as MFI in unstimulated and stimulated cells.

In vitro R848 treatment of murine splenocytes

$CD4^+$ splenocytes were isolated through magnetic bead sorting (LT34; Miltenyi Biotec) from 10 untreated C57BL/6 mice (6–8 wk old). Briefly, flat-bottom 96-well plates were coated for 4 h at 37°C with 2 μg/ml anti-CD3E (145-2C11; BioLegend) and 2 μg/ml anti-CD28 (37.51; BioLegend) Abs. Total $CD4^+$ or sorted naive $CCR6^-$, memory $CCR6^-$, and memory $CCR6^+CD4^+$ splenocytes were seeded at 5×10^4 cells/well in complete medium (RPMI 1640 supplemented with 10% FCS, 1× nonessential amino acids, 1 mM sodium pyruvate, 20 mM GlutaMAX, 50 μM 2-ME, 50 U/ml penicillin, and 50 μg/ml streptomycin) in the presence or absence of 1 μg/ml R848. After 72 h, cell migration induced by murine CCL20 (described in *Chemotaxis assay*), proliferation, apoptosis, and CCR6 expression in $CCR6^+$ and $CCR6^-$ subpopulations were assessed.

Cell proliferation was evaluated by the CFSE dilution method. Briefly, total $CD4^+$ splenocytes were stained with 2.5 μM CFSE, using the CellTrace CFSE cell proliferation kit (C34554; Invitrogen Molecular Probes) according to the manufacturer's instructions. After 72 h, cells were stained for 30 min at 4°C with the anti–CCR6-PE (29-2L17; BioLegend) Ab and acquired with a BD LSRFortessa (BD Biosciences). Frequency of proliferating cells was determined in $CCR6^+$ and $CCR6^-$ populations. Apoptosis was evaluated by flow cytometric determination of annexin V staining in the $CCR6^+$ and $CCR6^-$ populations. Briefly, total $CD4^+$ splenocytes were stained for 30 min at 4°C with the anti–CCR6-PE (29-2L17; BioLegend) Ab. After surface staining, cells were stained with annexin V–FITC in 1× binding buffer (10 mM HEPES [pH 7.4], 140 mM NaOH, 2.5 mM $CaCl_2$) for 15 min at room temperature in the dark and acquired with a BD LSRFortessa (BD Biosciences).

Statistical analysis

Data are presented as mean ± SEM. The statistical significance between two groups was determined using a nonparametric two-tailed Mann–Whitney *U* test or a paired *t* test. The statistical significance between more than two groups was evaluated using a Kruskal–Wallis test followed by a Dunn multiple comparison adjustment, or two-way ANOVA followed by a Bonferroni adjustment where appropriate. Correlation was assessed using Spearman rank-order correlation. A p value <0.05 was considered statistically significant. Data were analyzed using GraphPad Prism version 5.0.

Results

$CCR6^+$ and $CXCR3^+$ Th cell dynamics in experimental SIV infection

To analyze the dynamics of $CCR6^+$ and $CXCR3^+$ Th cells during the course of SIV infection, we have assessed their frequency by flow cytometry in a cohort of uninfected and SIV-infected rhesus macaques either at the postacute set point or in the chronic phase of infection. The frequency of circulating $CCR6^+$ and $CXCR3^+$ Th cells declined very rapidly during the course of infection (Fig. 1A). Later on, during the chronic phase, $CD4^+$ T cells remained low, whereas $CCR6^+$ and $CXCR3^+$ Th cells tended to recover (Fig. 1A), and all frequencies were negatively correlated with plasma viral load (Fig. 1B).

Interestingly, circulating $CCR6^+$ and $CXCR3^+$ cells from SIV-infected macaques poorly migrated in response to the selective chemokines CCL20 and CXCL10 both in the acute and in the chronic phase of infection (Fig. 1C). Of note, this reduction was not related to the expression of chemokine receptors on cell surface, as no changes during infection were detected for CCR6, whereas the expression of CXCR3 was diminished only during the acute phase and subsequently recovered (Fig. 1D).

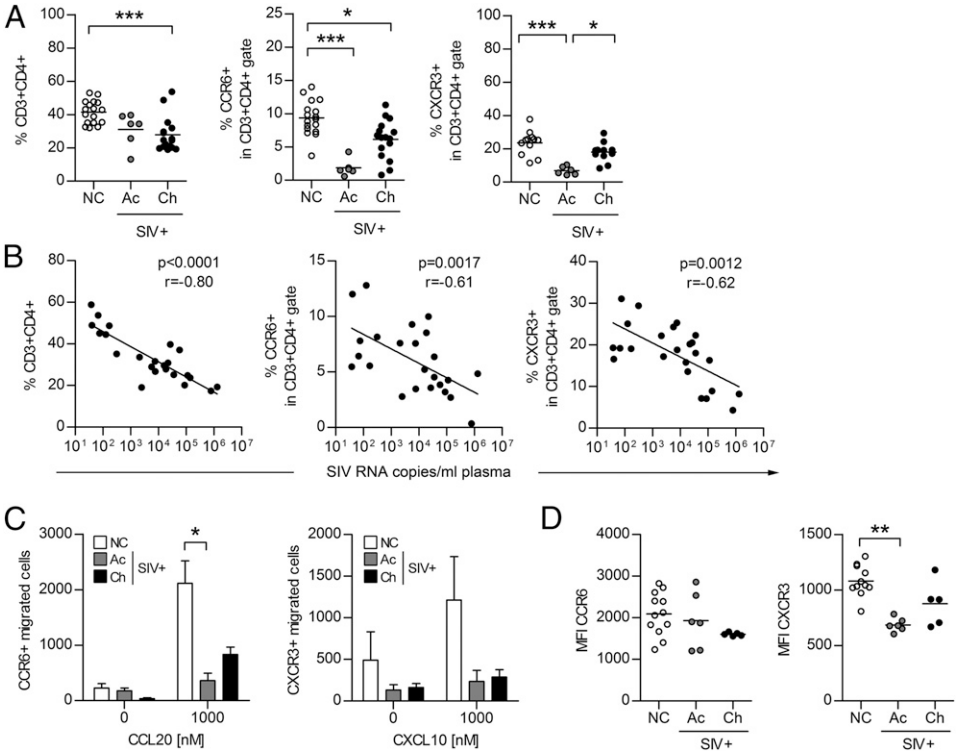

FIGURE 1. $CCR6^+$ and $CXCR3^+$ Th cell frequencies during experimental SIV infection. (**A**) Frequency of circulating $CD3^+CD4^+$, $CCR6^+CD4^+$, and $CXCR3^+CD4^+$ T cells in 17 uninfected normal controls (NC) or 22 SIV-infected macaques, either in the postacute (Ac, $n = 6$) or in the chronic (Ch, $n = 16$) phase of infection. (**B**) Correlation analysis between plasma viral load at week 16 postinfection and the frequency of $CD3^+CD4^+$, $CCR6^+CD4^+$, and $CXCR3^+CD4^+$ T cells in 24 chronically infected macaques. Data were analyzed using the Spearman rank correlation method, and p and r values are indicated in the figure for each plot. (**C**) Migration induced by CCL20 or CXCL10 in $CCR6^+$ or $CXCR3^+$ cells from uninfected normal controls (NC, $n = 5$), and SIV-infected macaques in the postacute (Ac, $n = 3$) or in the chronic (Ch, $n = 5$) phase of infection. Means ± SEM of migrated cells are shown. (**D**) CCR6 or CXCR3 expression on total lymphocyte measured by flow cytometry in uninfected normal controls (NC, $n = 11$) or SIV-infected macaques in the postacute (Ac, $n = 6$) or chronic (Ch, $n = 5$) phase of infection. Horizontal bars represent the mean value. $^*p < 0.05$, $^{**}p < 0.01$, $^{***}p < 0.001$ by Kruskal–Wallis test with a multicomparison Dunn adjustment (A, C, and D).

Immunohistochemical analysis of the colonic lamina propria from SIV-infected macaques, performed on serial tissue sections, confirmed intestinal $CD4^+$ cell depletion during the course of infection, and it revealed that this was paralleled by a decrease of $CCR6^+$ cells (Fig. 2A). The expression of CCL20, the selective CCR6 agonist, was not downmodulated during the infection and was mainly observed in the epithelial layer (Fig. 2B). Both $CD3^+$ and $CXCR3^+$ cells were significantly increased in the chronic phase of infection, most likely accounting for $CD8^+CXCR3^+$ T cells recruited by CXCL10, a selective chemokine for CXCR3, which was also found to be expressed in the lamina propria of SIV-infected macaques (Fig. 2).

$CCR6^+$ and $CXCR3^+$ Th cell dynamics in HIV-1 infection: effect of ART

To analyze the effect of ART on the dynamics of circulating $CCR6^+$ and $CXCR3^+$ Th cells during the course of HIV-1 infection, we studied untreated and ART-treated patients from the SHCS. A total of 58 patients were enrolled in the study and divided into three groups according to their therapeutic regimen and CD4 nadir. Untreated HIV-1–infected patients were represented in group A, whereas patients under long-term ART (>3 y) were allocated to groups B and C and divided according to the level of immunodeficiency reached (CD4 nadir of <100 cells/μl or >350 cells/μl of blood, respectively). Patients were characterized for treatment, absolute CD4 counts in blood, plasma viral load, and distribution of $CD4^+$ naive, central memory, and effector memory T cells at the time when the specimen was taken for further analyses (Supplemental Fig. 1B, 1C, Table I).

A significant increase in the frequency of circulating $CCR6^+$ Th cells was found in group B as compared with HD, and indeed the absolute number of these cells increased in all patients under long-term ART, reaching significance in patients from group C (Fig. 3A, Supplemental Fig. 1D). Moreover, similar results were observed in the frequency and absolute number of $CXCR3^+$ Th cells (Fig. 3B, Supplemental Fig. 1E). In untreated HIV-1–infected patients from group A, regression analysis using the Spearman rank correlation method showed that plasma viral load negatively correlated with the frequency of total $CD4^+$ T cells ($p = 0.0055$, $r = -0.69$), but not with the frequency of $CD4^+$ Th cells expressing either CCR6 ($p = 0.49$) or CXCR3 ($p = 0.97$) (data not shown).

Significantly higher levels of sCD14 were found in the plasma of ART-treated HIV-1–infected patients as compared with HD, indicating persistence of immune activation (Fig. 3C), which is not abolished in the absence of circulating virus. Of note, no correlation was found between sCD14 and the frequency of circulating $CD4^+$ Th cells ($p = 0.64$, $r = -0.14$), whereas sCD14 positively correlated with the frequencies of $CCR6^+$ and $CXCR3^+$ Th cells (Fig. 3D), showing a higher significance in the pool of central memory T cells (Fig. 3E).

Impairment of cell migration is maintained in ART-treated HIV-1–infected individuals

Given the impairment in cell migration observed in the untreated SIV infection model, we decided to analyze the migratory capacity of circulating $CCR6^+$ and $CXCR3^+$ Th cells that accumulate in the blood of ART-treated patients.

Circulating $CCR6^+$ and $CXCR3^+$ cells from HIV-1–infected patients showed, similar to what was observed in SIV-infected macaques, a strong impairment in the response to both CCL20 and CXCL10. Most importantly, ART did not improve the ability of $CCR6^+$ cells to respond to CCL20, nor of $CXCR3^+$ cells to respond to CXCL10, suggesting that long-term efficient reduction in viral load to mostly undetectable levels is not sufficient to restore the ability of these cells to respond to chemotactic stimuli (Fig. 3F, Supplemental Fig. 2A). Cell migration impairment in response to CCL20 was mostly affecting $CD4^+$ T cells, whereas $CD8^+$ T cell migration was decreased only in HIV-1–infected patients from group B (Supplemental Fig. 2B). As observed in SIV infected macaques, no changes were found in the expression of CCR6 and CXCR3 in cells from HIV-1–infected patients compared with HD (Fig. 3G). In vitro cell tracking showed that $CCR6^+$ Th cells from HD, exposed to plasma from aviremic HIV-1–infected patients under ART, randomly moved significantly slower on fibronectin compared with exposure to HD plasma (Fig. 3H).

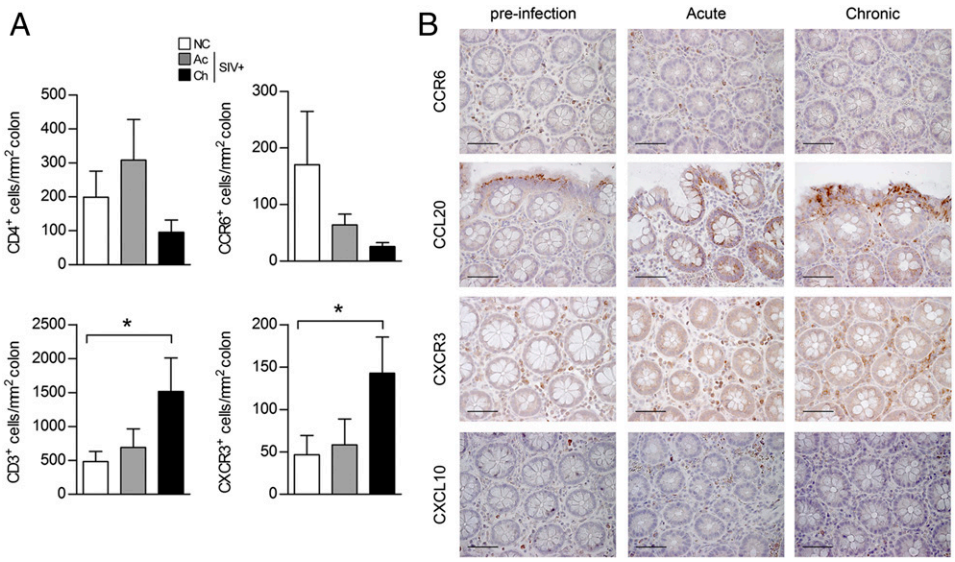

FIGURE 2. Reduced number of $CCR6^+$ cells in the gut lamina propria of SIV-infected macaques. (**A**) Quantification of $CD4^+$, $CD3^+$, $CCR6^+$, and $CXCR3^+$ cells in the colon of three SIV-infected macaques at different time points during infection (normal controls [NC], preinfection; acute [Ac] infection, 10 d postinfection; chronic [Ch] infection, 13 wk postinfection). Data are presented as means ± SEM. (**B**) Immunohistochemical staining of CCR6, CCL20, CXCR3, and CXCL10 in colon biopsies from three SIV-infected macaques at different time points during infection. Positive cells, detected with the diaminobenzidine substrate, are shown in brown. One representative image for each staining is shown. Original magnification, ×40; scale bar, 200 μm. *$p < 0.05$ by Kruskal–Wallis test with a multicomparison Dunn adjustment (A).

Table I. HIV-1–infected patients included in the study

Patient ID	ART	Absolute CD4 (Cells/μl Blood)	Viral Load (mRNA Copies/ml Plasma)	Age (y)	Sex
Group A					
PT-1	No	663	93,685	41	M
PT-2	No	584	3,306	53	M
PT-3	No	581	89,386	32	M
PT-4	No	482	45,332	34	F
PT-5	No	1621	4,229	35	M
PT-6	No	525	66,325	31	M
PT-7	No	462	25,490	24	M
PT-8	No	361	18,119	41	F
PT-9	No	820	14,115	28	M
PT-10	No	1269	197	61	M
PT-11	No	688	0	54	F
PT-12	No	189	228,635	49	M
PT-13	No	1162	0	51	M
PT-14	No	289	171,400	55	M
PT-15	No	695	11,412	51	M
Group B[a]					
PT-16	Yes	657	0	57	M
PT-17	Yes	579	0	35	F
PT-18	Yes	212	0	56	F
PT-19	Yes	247	0	40	M
PT-20	Yes	803	0	47	M
PT-21	Yes	500	0	51	M
PT-22	Yes	827	0	69	M
PT-23	Yes	1097	0	51	M
PT-24	Yes	678	0	49	M
PT-25	Yes	331	0	40	M
PT-26	Yes	378	93	47	M
PT-27	Yes	369	0	51	M
PT-28	Yes	435	69	50	M
PT-29	Yes	772	0	48	F
PT-30	Yes	840	0	49	M
PT-31	Yes	318	0	45	M
PT-32	Yes	684	0	50	M
PT-33	Yes	388	0	79	M
PT-34	Yes	400	0	53	M
PT-35	Yes	203	0	79	M
PT-36	Yes	559	0	49	F
PT-37	Yes	359	0	62	M
PT-38	Yes	870	34	51	M
PT-39	Yes	512	0	67	M
PT-40	Yes	381	0	61	M
PT-41	Yes	558	0	63	M
PT-42	Yes	337	0	53	M
PT-43	Yes	786	0	42	F
PT-44	Yes	629	0	71	M
Group C[b]					
PT-45	Yes	843	0	46	M
PT-46	Yes	2176	0	44	F
PT-47	Yes	1020	22	45	M
PT-48	Yes	798	0	51	M
PT-49	Yes	629	<20	37	M
PT-50	Yes	905	0	53	M
PT-51	Yes	915	0	61	M
PT-52	Yes	586	0	55	M
PT-53	Yes	823	0	44	M
PT-54	Yes	644	0	42	M
PT-55	Yes	816	4,653	40	M
PT-56	Yes	786	0	56	M
PT-57	Yes	963	0	41	M
PT-58	Yes	877	0	40	M

Demographic characteristics, treatment, absolute CD4 counts in blood, and plasma viral load of the 58 HIV-1–infected individuals enrolled in the study are shown.

[a]CD4 nadir of <100 cells/μl of blood.

[b]CD4 nadir of >350 cells/μl of blood.

In line with the finding that CCL20 production at mucosal sites is maintained during SIV infection (Fig. 2B), mo-DCs from HIV-1–infected patients retained their capacity to secrete both CCL20 and CXCL10 following LPS or *Candida albicans* stimulation (Supplemental Fig. 2C).

Cytoskeleton machinery impairment in HIV-1 infection is rescued by OA

We analyzed the ability of $CCR6^+$ and $CXCR3^+$ cells from HD and the three groups of HIV-1–infected patients to polymerize actin, which is an essential process during cellular migration. The levels of intracellular F-actin in both $CCR6^+$ and $CXCR3^+$ cells were significantly lower in HIV-1–infected patients compared with HD, both at the basal level and following chemokine stimulation (Fig. 4A). Although cells from patients were able to respond to the stimuli, actin polymerization in HIV-1–infected patients, and in particular in the ART-treated ones from group B ($p < 0.05$, Fig. 4B), was lower compared with HD. This might indicate that, after stimulation, the threshold required to induce an effective migration is not reached by the cells from the patients.

HIV-1 is able to hijack the cellular cytoskeleton machinery to increase viral entry and integration in the host genome (48, 49). In particular, the viral protein nef from HIV-1 has been shown to inhibit cofilin activity, thus reducing actin polymerization turnover (50). In the samples we analyzed, *nef* mRNA was not detectable, neither in viremic nor in ART-treated HIV-1–infected patients (data not shown); on the contrary, a significant increase of total and phosphorylated cofilin was found in lymphocytes from HIV-1–infected patients compared with HD (Fig. 4C). Interestingly, the ratio of phosphorylated cofilin over total cofilin was significantly lower in lymphocytes from HIV-1–infected patients compared with HD, thus indicating a higher activity of the protein during HIV-1 infection (Fig. 4D), with no differences between untreated and treated individuals (data not shown). The increase in the total amount of cofilin was not due to an upregulation of its mRNA level (Fig. 4E). These data indicate a higher and not efficient actin polymerization turnover, resulting in inefficient response to chemotactic stimuli.

On the basis of the above results, we decided to promote actin polymerization by using OA, a toxin able to induce cytoskeleton reorganization, also by activating LIM kinase-1, which is responsible for turning off cofilin activity (51). In vitro OA treatment was able to rescue F-actin formation (Fig. 4F) and most importantly cell migration (Fig. 4G) of both $CCR6^+$ and $CXCR3^+$ cells from HIV-1–infected patients (group B), without altering the response to these chemokines in cells from HD (Supplemental Fig. 3), pointing out a direct effect of cofilin in dampening the response to chemokines in HIV-1 infection.

Chronic immune activation reduces Th cell migration both in vitro and in vivo

Chronic immune activation is a common feature of both treated and untreated HIV-1 infection. Therefore, it could account for the impaired cell migration that we have found, despite ART therapy, in all groups of HIV-1–infected patients. To assess this hypothesis, we used an established in vivo model (14) to mimic chronic immune activation by systemically injecting the TLR7/8 agonist R848 in C57BL/6 mice. The treatment induced a significant increase in the frequency of circulating $CCR6^+$ Th cells, but it did not affect circulating $CXCR3^+$ and $CXCR4^+$ Th cells (Fig. 5A). $CCR6^+$ Th cells isolated from the spleen poorly migrated in response to CCL20, despite a similar CCR6 expression in treated and untreated animals (Fig. 5B). To verify whether the impairment occurs before an evident accumulation of circulating Th cells, and whether it is selective for $CCR6^+$ Th cells, we next analyzed the response to a receptor, CXCR4, which is broadly expressed by leukocytes. Similar to what we observed for $CCR6^+$ Th cells, total $CD4^+$ T cell migration in response to CXCL12 was reduced, but it

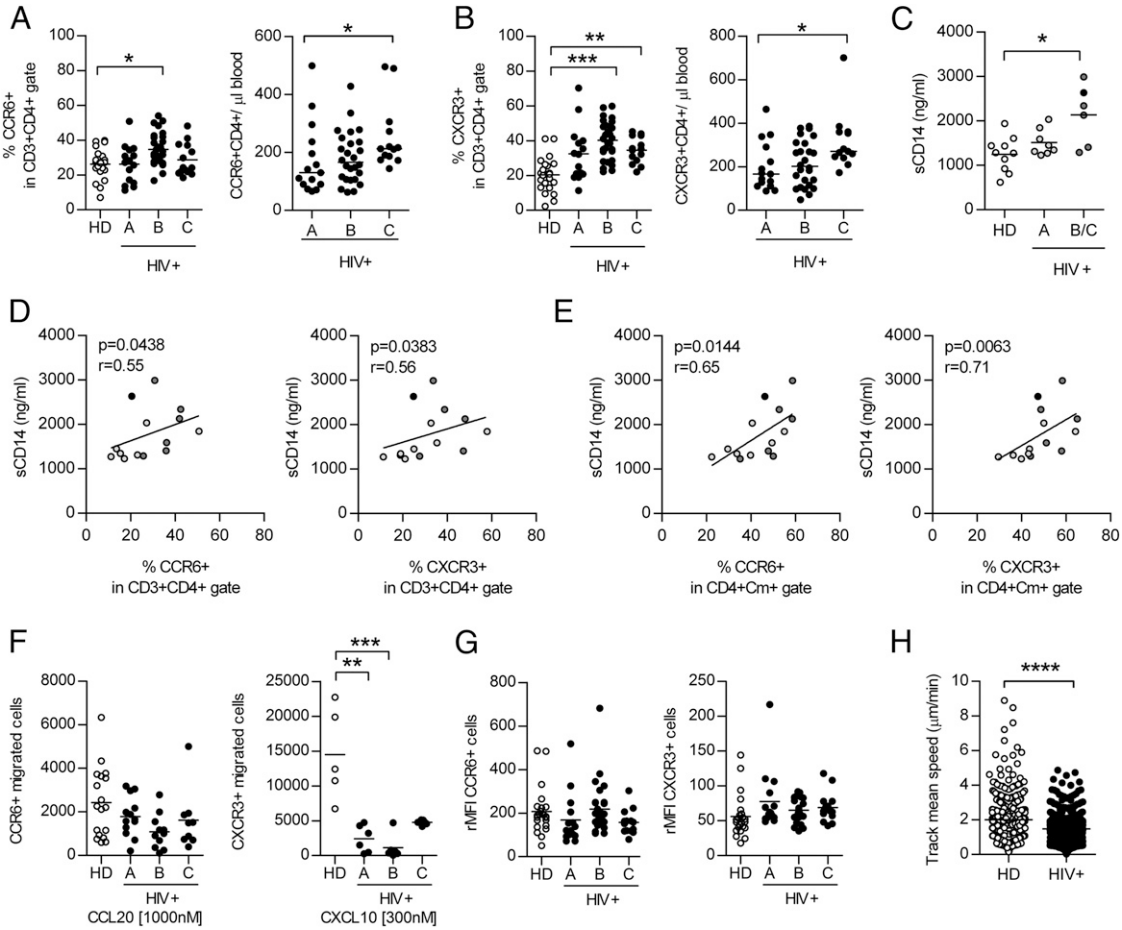

FIGURE 3. CCR6$^+$ and CXCR3$^+$ Th cells accumulate in the blood during HIV-1 infection and poorly migrate in response to CCL20 or CXCL10. Th cells in the blood of 23 HD and 58 HIV-1–infected patients from the three groups were analyzed. (**A** and **B**) Frequency and absolute numbers of circulating CCR6$^+$CD4$^+$ (A) or CXCR3$^+$CD4$^+$ T cells (B). (**C**) Concentration of sCD14 in the plasma of 10 HD and 14 HIV-1–infected individuals from the three groups [(A), $n = 8$; (B), $n = 5$; (C), $n = 1$]. (**D** and **E**) Correlation analysis between plasma levels of sCD14 and the frequency of total (D) or central memory (Cm) (E) CCR6$^+$ or CXCR3$^+$ Th cells in 14 HIV-infected individuals from the three groups [(A), light gray; (B), dark gray; (C), black]. Data were analyzed using the Spearman rank correlation method, and p and r values are indicated in the figure for each plot. (**F**) Migration of CCR6$^+$ and CXCR3$^+$ cells at optimal concentrations of CCL20 or CXCL10, respectively, in at least 5 HD and 19 HIV-1–infected patients. Horizontal bars represent the mean value. (**G**) CCR6 and CXCR3 expression on total lymphocytes measured by flow cytometry in 23 HD and in 58 HIV-1–infected patients. Horizontal bars represent the mean value. rMFI represents the ratio between stained and unstained samples. (**H**) Track mean speed of lymphocytes isolated from HD and exposed to plasma from HD or HIV-1$^-$infected patients (HIV$^+$). One representative out of three experiments performed with cells from different donors is shown. Horizontal bars represent the mean value. $^*p < 0.05$, $^{**}p < 0.01$, $^{***}p < 0.001$ by Kruskal–Wallis test with a multicomparison Dunn adjustment (A, B, F, and G), nonparametric two-tailed Mann–Whitney U test (C and H).

was not ascribed to downmodulation of CXCR4 on the cell surface (Fig. 5C). The accumulation of CCR6$^+$ Th cells observed in the blood of treated mice was not due to a direct effect of R848 on apoptosis of CCR6$^-$ cells, proliferation of CCR6$^+$ cells, or induction of CCR6 expression in the CCR6$^-$ population (Supplemental Fig. 4A–C). Of note, CCR6$^+$ Th cells, isolated from the spleen of untreated mice, lost their ability to migrate in response to CCL20 when stimulated in vitro with R848 (Supplemental Fig. 4D).

The analysis of the PP from treated mice revealed a significant decrease in the total cell number, as well as in CD4$^+$ Th cells (Fig. 6A), which was associated with a significant reduction of CCR6$^+$ cells as assessed by immunohistochemistry (Fig. 6B). These data further corroborate the hypothesis that impairment in cell migration may account for the reduced T cell numbers in the gut mucosa, and that this impairment is due to chronic immune activation, in addition to a direct effect of the virus. Similar to the data obtained with cells from HIV-1–infected patients, OA was able to partially restore in the R848-treated mice the migration of both total CD4$^+$ and CCR6$^+$ Th cells (Fig. 6C).

To assess whether OA can modulate the effect of chronic immune activation on cell migration in vivo, air pouches were generated in R848-treated and untreated mice and, given the low frequency of CCR6$^+$ Th cells present in the circulation of mice housed in specific pathogen-free conditions, we measured the number of CD4$^+$ T cells recruited in response to CXCL12. As observed in the in vitro experiments, CD4$^+$ T cells of treated mice were not able to efficiently respond to the chemokine. Strikingly, this impairment was rescued by the injection of OA together with CXCL12 in the air pouches (Fig. 6D), indicating that the drug injected at the abluminal sites can favor, similar to the in vitro experiments, a cytoskeleton remodeling of the leading edge in cells patrolling the skin endothelium. This was sufficient to restore T cell capacity to respond to chemotactic cues.

Discussion

The dynamics of different subsets of circulating Th cells in the course of HIV-1 infection have been widely investigated with the help of the expression of specific tissue-homing markers. Nevertheless, a

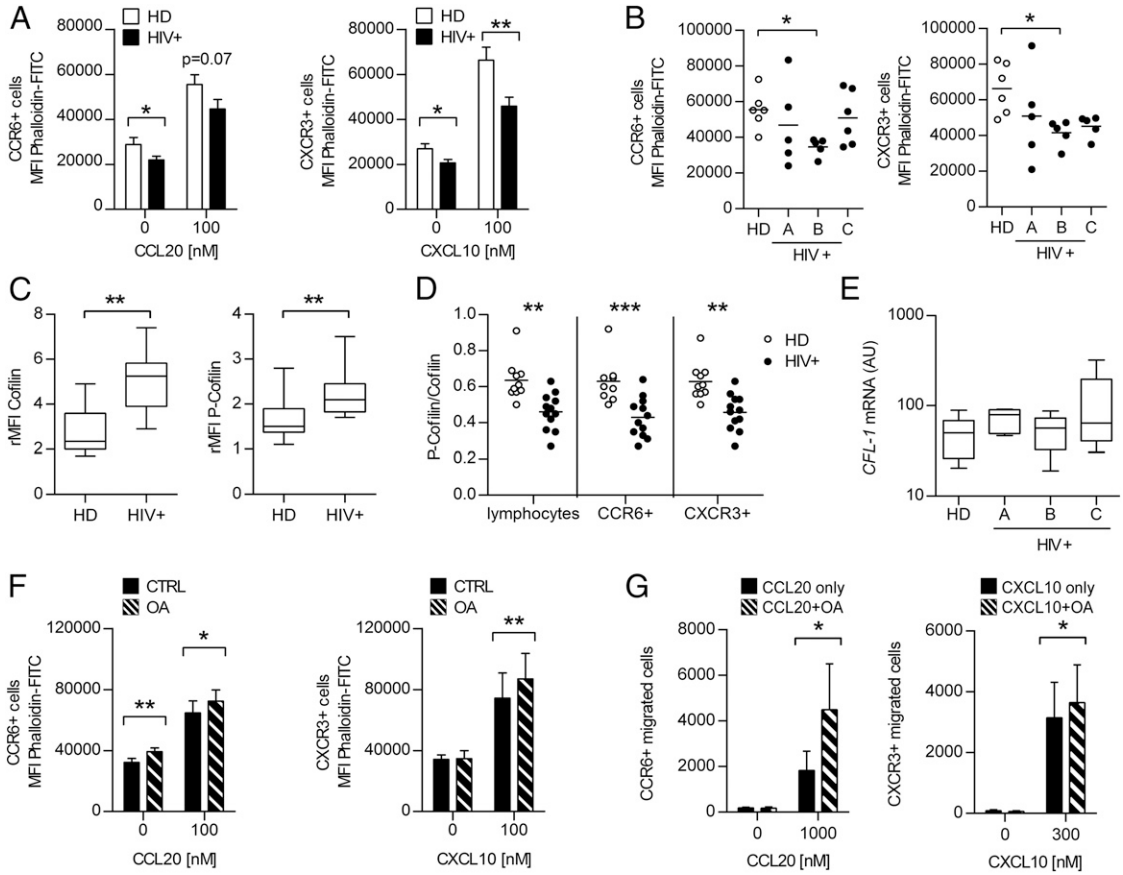

FIGURE 4. Reduced levels of actin polymerization are associated with increased activity of cofilin in lymphocytes from HIV-1–infected patients and are restored by OA. (**A** and **B**) Actin polymerization in lymphocytes isolated from 6 HD and 15 HIV-1–infected patients from the three groups [(A), $n = 5$; (B), $n = 5$; (**C**), $n = 5$]. F-actin was measured as phalloidin-FITC MFI in cells untreated or treated for 15 s with CCL20 or CXCL10, respectively. Data are presented as means ± SEM of untreated and treated cells (A), whereas (B) shows the single values of treated cells in the different groups of patients. (C) Expression of cofilin and P-cofilin measured by flow cytometry in total lymphocytes from 10 HD and 12 HIV-1–infected patients from groups A ($n = 5$) and C ($n = 7$). Box plots: minimum to maximum. rMFI represents the ratio between stained and unstained samples. (**D**) Cofilin activity in lymphocytes, measured as the ratio of P-cofilin over total cofilin in 10 HD and 12 HIV-1–infected patients from groups A ($n = 5$) and C ($n = 7$). Horizontal bars represent the mean value. (**E**) mRNA expression of cofilin (*CFL-1*) in total PBMCs from HD and from HIV-1–infected patients. Values are presented as arbitrary units (AU) over 18 s from five samples in each group. (**F**) Actin polymerization in lymphocytes isolated from HIV-1–infected patients from group B and preincubated in the absence (control [CTRL]) or presence of OA. F-actin content was measured as in (A), and data are presented as means ± SEM from at least three independent experiments. (**G**) Migration of lymphocytes isolated from HIV-1–infected patients from group B in response to the indicated chemokines, either alone or in combination with OA. Data are presented as means ± SEM of migrated cells of five independent experiments. $*p < 0.05$, $**p < 0.01$, $***p < 0.001$ by nonparametric two-tailed Mann–Whitney *U* test (A, C, and D), Kruskal–Wallis test with a multicomparison Dunn adjustment (B and E), paired *t* test (F and G).

functional analysis on Th cell ability to respond to selective chemokine receptor agonists is missing. For the first time, to our knowledge, we have elucidated the relationship among the degree of immunodeficiency, cell recovery following ART treatment, and the ability of Th cells to respond to chemoattractants. This study discloses a novel path occurring in viral infection that, after the clearance of circulating virus, can impair the host immune system.

We show that $CCR6^+$ and $CXCR3^+$ Th cells accumulate in the blood of ART-treated HIV-1–infected patients, and their frequencies correlate with a status of chronic immune activation. Cell accumulation is most likely due to their incompetence to respond to chemokines, thus preventing their trafficking to peripheral organs. Although the impaired migration of Th cells is a common feature of both SIV and HIV-1 infection, their accumulation in the blood becomes evident only in patients successfully treated by ART. Regardless of therapy, circulating lymphocytes from HIV-1–infected patients, which show a compromised migration, are characterized by inefficient actin polymerization in response to chemotactic stimuli and express high levels of active cofilin, which contribute to an increased process of F-actin severing. By modulating the cytoskeleton activity, we were able to rescue both optimal levels of intracellular F-actin and efficient cell migration following chemokine receptor triggering. For the first time, to our knowledge, we show in a mouse model that mimics the immunological alterations observed in HIV-1 infection (14) that chronic immune activation leads to $CCR6^+$ Th cell accumulation in the circulation. This is associated with a reduced number of $CD4^+$ T cells in the PP, as well as an impairment of lymphocyte migration that can be reverted by modulating the cytoskeleton activity.

In untreated HIV-1–infected patients, and in line with previously published data (29, 52), we show a significant decrease in the frequency of $CD4^+CCR6^+$ effector memory T cells, which speaks for this cell type being a major target for HIV-1 (29, 31). The present study shows that, although the frequency of central memory $CCR6^+$ T cells increased in patients with a low (<100 cells/μl of blood, group B) and high (>350 cells/μl of blood, group C) CD4 nadir, the highest numbers of circulating $CCR6^+$ Th cells were found in patients with a high CD4 nadir (Supplemental Fig. 1D). Indeed, in the

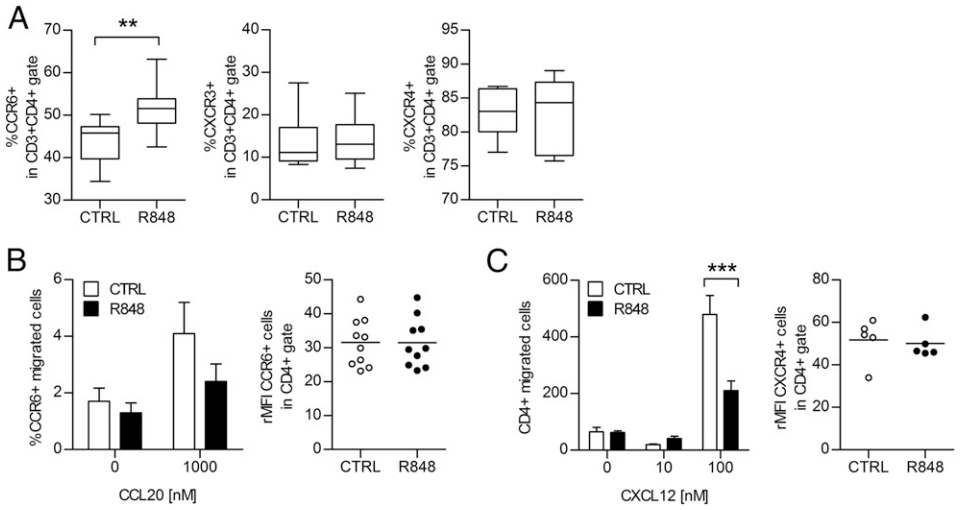

FIGURE 5. In vivo chronic immune activation reduces lymphocyte migration induced by chemokines. (**A**) Frequency of circulating CCR6$^+$, CXCR3$^+$, and CXCR4$^+$ Th cells in at least five controls (CTRL) and five R848-treated mice. Box plots: minimum to maximum. (**B**) Left panel, Migration of CCR6$^+$ cells isolated from the spleen of five CTRL or five R848-treated mice, in response to murine CCL20. Values were calculated as the percentage of CCR6$^+$ cells migrated in comparison with the actual input of CCR6$^+$ cells. Means ± SEM of migrated cells are shown. Right panel, CCR6 expression on Th cells (rMFI) in CTRL and in R848-treated mice. Horizontal bars represent the mean value. rMFI represents the ratio between stained and unstained samples. (**C**) Left panel, Migration of CD4$^+$ cells isolated from the spleen of five controls or five R848-treated mice in response to murine CXCL12. Means ± SEM of migrated cells are shown. Right panel, CXCR4 expression on Th cells (rMFI) in CTRL and in R848-treated mice. Horizontal bars represent the mean value. rMFI represents the ratio between stained and unstained samples.$^{**}p < 0.01$, $^{***}p < 0.001$ by nonparametric two-tailed Mann–Whitney *U* test (A–C), two-way ANOVA with a Bonferroni adjustment (B and C). CTRL, control.

absence of circulating virus, CCR6$^+$ Th cells can be generated but accumulate in the bloodstream of ART-treated patients. Regarding CXCR3$^+$ Th cells, we found a significant increase in their frequency both in untreated and treated patients, regardless of their CD4 nadir, thus confirming the data from Gosselin et al. (29) and indicating that they are not a primary target for HIV-1 (29, 31).

Mavigner et al. (53) have shown an accumulation of CCR9$^+$ Th cells in the circulation of ART-treated patients and suggested that, due to a decrease in the expression of the attracting chemokine CCL25 in the epithelium of the intestine, T cells coming into the gut are reduced, thus preventing a complete repopulation of this tissue. Our data on SIV-infected macaques suggest that during untreated infection the loss of CCR6$^+$ cells in the intestine is the consequence of a combination of both direct viral cytotoxicity and inefficient response to chemokines, which prevents homing to the gut and is not associated with a decrease in mucosal CCL20 production or downmodulation of CCR6 expression. Indeed, no changes in CCL20 expression in the intestine of SIV-infected macaques were reported in a previous study (54). The altered response to chemokines that we have also observed in ART-treated, aviremic patients might contribute to inefficient cell migration into the intestine, thus preventing a complete repopulation of this compartment.

Inefficient cell migration is not specific for CCR6$^+$ cells, but it could be the outcome of a more generalized impairment in lymphocyte trafficking. We also show that CXCR3$^+$ cells, both from SIV-infected macaques and HIV-1–infected patients, are not able to efficiently respond to CXCL10 in vitro, and this is again not due to changes in receptor expression. This hypothesis is further supported by the work from Perez-Patrigeon et al. (55) who have shown a reduction in the migration of T cells expressing CCR7 in HIV-1–infected patients, despite normal levels of the chemokine receptor expression. The increased number of CD8$^+$CXCR3$^+$ cells in the intestine of untreated SIV-infected animals suggests that CD8$^+$ cells are still able to home to the gut despite persistent immune activation and high viral load. Our data on CCR6$^+$ cells from HIV-1-infected patients argue for a different migratory impairment of CD4$^+$ versus CD8$^+$ cells (Supplemental Fig. 2B), and they call for further studies assessing differences in response to selective chemokines.

The molecular mechanisms responsible for these observed impairments are far from being fully elucidated. Overexpression of the viral protein nef, by reducing cofilin activity, inhibits dynamic actin remodeling, thus reducing cellular migration both in vitro and in vivo (50, 56). Cofilin and the actin pathways are also directly modulated by HIV-1 *gp120* that, by triggering CXCR4, is able to hijack the cytoskeleton machinery, favoring viral entry and integration into the host genome (48, 51, 57). We show ex vivo that cofilin activity is increased, rather than reduced, in all groups of HIV-1–infecetd patients. Its activation is associated with impairment in actin polymerization, both at the basal level and upon chemokine receptor engagement, and it is not related to *nef* expression. Wu et al. (58) also showed increased cofilin activity in T cells from ART-treated patients, and they suggested its direct involvement in the abnormal T cell homing and migration observed in HIV infection. Our data further support the hypothesis that effective ART, despite suppressing plasma viral load and increasing the number of circulating Th cells, is not able to fully restore Th cell functions. Of note, exposure of CD4$^+$CCR6$^+$ cells from healthy donors to plasma from ART-treated patients with undetectable viral load is sufficient to reduce cell movement. Further studies assessing the activity of sera from patients with persistent viral infections are needed to identify the factor responsible for this impairment and to determine whether this is a common feature of diseases characterized by chronic immune activation.

In this study we prove that optimal levels of actin polymerization and efficient cell migration can be restored in cells from HIV-1–infected patients by modulating the pathway leading to actin polymerization with OA, thus establishing the missing link between aberrant cofilin activation and reduced T cell migration. OA represents a useful tool for modulating actin polymerization in vitro, but its usage in vivo is limited due to its high toxicity.

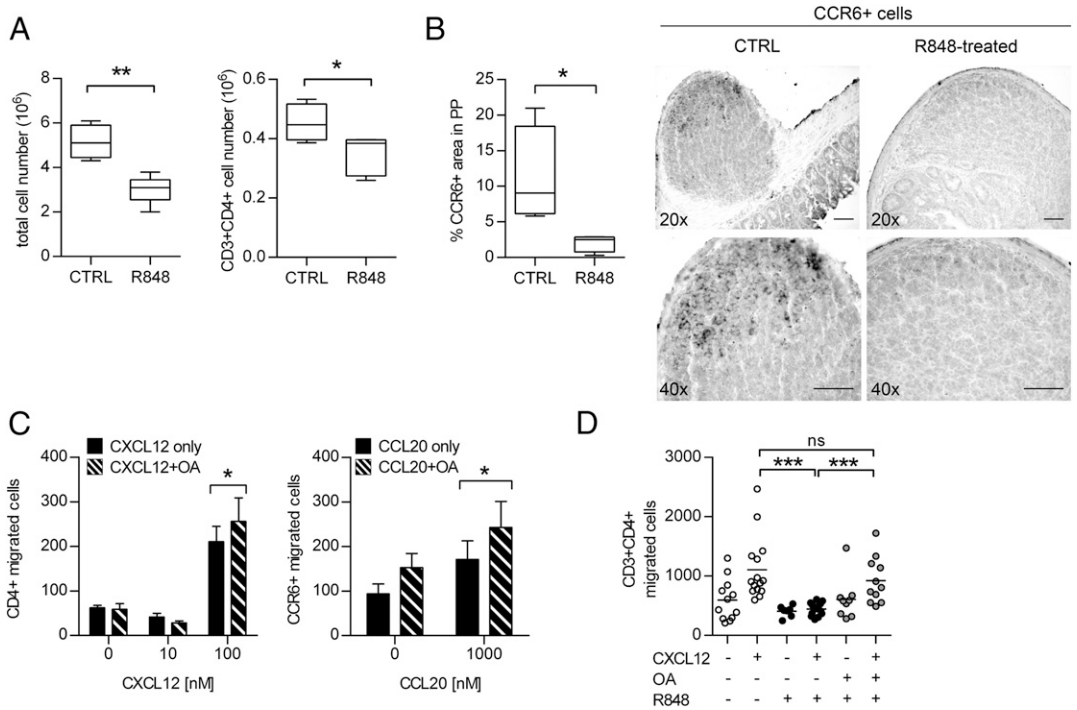

FIGURE 6. OA rescues lymphocyte migration induced by chronic immune activation both in vitro and in vivo. (**A**) Absolute number of total or $CD4^+$ Th cells in PP in at least five controls (CTRL) and five R848-treated mice. Box plots: minimum to maximum. (**B**) Immunohistochemical staining of CCR6 in PP from five CTRL and five R848-treated mice. Data are expressed as percentage of $CCR6^+$ area in PP. Box plots: min to max. One representative image each is shown. Original magnification, ×20 and ×40; scale bar, 200 μm. Positive cells are shown in black. (**C**) Migration of $CD4^+$ cells isolated from the spleen of R848-treated mice in response to the indicated murine chemokines, either alone or in combination with OA. Means ± SEM of migrated cells in five independent experiments are shown. (**D**) CXCL12-induced recruitment in vivo of $CD4^+$ Th cells into the air pouches of controls (open circles), and R848-treated mice in the absence (black circles) or presence (gray circles) of OA. Horizontal bars represent the mean value. $*p < 0.05$, $**p < 0.01$, $***p < 0.001$ by nonparametric two-tailed Mann–Whitney *U* test (A), two-way ANOVA with a Bonferroni adjustment (B), Kruskal–Wallis test with a multicomparison Dunn adjustment (C). CTRL, control.

Increasing evidence shows that not only persistent viral ssRNA, but also ssRNA and DNA from a variety of pathogens, including bacteria, protozoa, and fungi, can be sensed by the host immune system through TLR7/8 and TLR9 triggering (59, 60). This triggering affects a variety of cells, leading to cytokine production and immune activation. Indeed, in the current paradigm of HIV-1–associated immune activation, indirect effects via triggering innate immune cells are essential for the development and maintenance of immune deficiency (61, 62). By taking advantage of an established murine model, which recapitulates chronic immune activation occurring in HIV-1 infection (14), we could prove that persistent immune activation via TLR7 triggering results in the retention of $CCR6^+$ Th cells in the bloodstream and in the impairment of lymphocyte response to chemotactic stimuli. Moreover, in treated mice the altered traffic to the mucosal compartment is highlighted by the reduction in both total and $CCR6^+$ cells present in the PP.

As proof of concept that efficient T cell migration can be restored by acting on the cytoskeleton, we used the air pouch model, which allows treatment with OA in a restricted skin area for a short period of time. We demonstrated that migratory capacity can be restored also in vivo, and we suggest how this model can be also developed for testing new compounds, with lower systemic toxicity, with the aim of targeting the cytoskeleton machinery in a number of diseases where chronic immune activation is part of the pathogenic features.

In conclusion, our findings imply a novel role for chronic immune activation during HIV-1 infection, which dampens the ability of leukocytes to respond to chemotactic stimuli, thus preventing a complete tissue reconstitution both in viremic and in ART-treated HIV-1–infected patients.

This study has many potential implications not only for the treatment of HIV-1–infected patients, but also for those experiencing persistent infections, which lead to chronic immune activation. Both in homeostasis and, for example, during vaccination protocols, it would be necessary to pharmacologically restore the capacity of their T cells to traffic to peripheral organs, and to reach niches able to support their maturation and subsequent functions.

Acknowledgments

We thank Beatrice Bernasconi and Christina Grube for excellent technical assistance, Enrica Mira-Catò and Luana Perlini for assisting in the experiments with mice, Rocco D'Antuono for assisting in the image analysis, and David Jarrossay for cell sorting.

Swiss HIV Cohort Study

Vincent Aubert, Manuel Battegay, Enos Bernasconi, Jürg Böni, Dominique L. Braun, Heiner C. Bucher, Alexandra Calmy, Matthias Cavassini, Angela Ciuffi, Günter Dollenmaier, Matthias Egger, Luigia Elzi, Jan Fehr, Jacques Fellay, Hansjakob Furrer (Chairman of the Clinical and Laboratory Committee), Christoph A. Fux, Huldrych F. Günthard (President of the SHCS), David Haerry (Deputy of the Positive Council), Barbara Hasse, Hans H. Hirsch, Matthias Hoffmann, Irene Hösli, Christian Kahlert, Laurent Kaiser, Olivia Keiser, Thomas Klimkait, Roger D. Kouyos, Helen Kovari, Bruno Ledergerber, Gladys Martinetti, Begona Martinez de Tejada, Catia Marzolini, Karin J. Metzner, Nicolas Müller, Dunja Nicca, Giuseppe Pantaleo, Paolo Paioni, Andri Rauch (Chairman of the Scientific Board), Christoph Rudin (Chairman of the Mother and Child Substudy), Alexandra U. Scherrer (Head of the Data Center), Patrick Schmid, Roberto F. Speck, Marcel Stöckle, Philip Tarr, Alexandra Trkola, Pietro Vernazza, Gilles Wandeler, Rainer Weber, and Sabine Yerly.

Disclosures

The authors have no financial conflicts of interest.

References

1. Veazey, R. S., M. DeMaria, L. V. Chalifoux, D. E. Shvetz, D. R. Pauley, H. L. Knight, M. Rosenzweig, R. P. Johnson, R. C. Desrosiers, and A. A. Lackner. 1998. Gastrointestinal tract as a major site of $CD4^+$ T cell depletion and viral replication in SIV infection. *Science* 280: 427–431.
2. Saharia, K. K., and R. A. Koup. 2013. T cell susceptibility to HIV influences outcome of opportunistic infections. *Cell* 155: 505–514.
3. Cao, J., I. W. Park, A. Cooper, and J. Sodroski. 1996. Molecular determinants of acute single-cell lysis by human immunodeficiency virus type 1. *J. Virol.* 70: 1340–1354.
4. Douek, D. C. 2003. Disrupting T-cell homeostasis: how HIV-1 infection causes disease. *AIDS Rev.* 5: 172–177.
5. Miedema, F., M. D. Hazenberg, K. Tesselaar, D. van Baarle, R. J. de Boer, and J. A. Borghans. 2013. Immune activation and collateral damage in AIDS pathogenesis. *Front. Immunol.* 4: 298.
6. Cecchinato, V., E. Tryniszewska, Z. M. Ma, M. Vaccari, A. Boasso, W. P. Tsai, C. Petrovas, D. Fuchs, J. M. Heraud, D. Venzon, et al. 2008. Immune activation driven by CTLA-4 blockade augments viral replication at mucosal sites in simian immunodeficiency virus infection. *J. Immunol.* 180: 5439–5447.
7. Liu, Z., W. G. Cumberland, L. E. Hultin, H. E. Prince, R. Detels, and J. V. Giorgi. 1997. Elevated CD38 antigen expression on $CD8^+$ T cells is a stronger marker for the risk of chronic HIV disease progression to AIDS and death in the multicenter AIDS cohort study than $CD4^+$ cell count, soluble immune activation markers, or combinations of HLA-DR and CD38 expression. *J. Acquir. Immune Defic. Syndr. Hum. Retrovirol.* 16: 83–92.
8. Giorgi, J. V., L. E. Hultin, J. A. McKeating, T. D. Johnson, B. Owens, L. P. Jacobson, R. Shih, J. Lewis, D. J. Wiley, J. P. Phair, et al. 1999. Shorter survival in advanced human immunodeficiency virus type 1 infection is more closely associated with T lymphocyte activation than with plasma virus burden or virus chemokine coreceptor usage. *J. Infect. Dis.* 179: 859–870.
9. Sandler, N. G., H. Wand, A. Roque, M. Law, M. C. Nason, D. E. Nixon, C. Pedersen, K. Ruxrungtham, S. R. Lewin, S. Emery, et al; INSIGHT SMART Study Group. 2011. Plasma levels of soluble CD14 independently predict mortality in HIV infection. *J. Infect. Dis.* 203: 780–790.
10. Foley, J. F., C. R. Yu, R. Solow, M. Yacobucci, K. W. Peden, and J. M. Farber. 2005. Roles for CXC chemokine ligands 10 and 11 in recruiting $CD4^+$ T cells to HIV-1-infected monocyte-derived macrophages, dendritic cells, and lymph nodes. *J. Immunol.* 174: 4892–4900.
11. Milush, J. M., K. Stefano-Cole, K. Schmidt, A. Durudas, I. Pandrea, and D. L. Sodora. 2007. Mucosal innate immune response associated with a timely humoral immune response and slower disease progression after oral transmission of simian immunodeficiency virus to rhesus macaques. *J. Virol.* 81: 6175–6186.
12. Qin, S., Y. Sui, A. C. Soloff, B. A. Junecko, D. E. Kirschner, M. A. Murphey-Corb, S. C. Watkins, P. M. Tarwater, J. E. Pease, S. M. Barratt-Boyes, and T. A. Reinhart. 2008. Chemokine and cytokine mediated loss of regulatory T cells in lymph nodes during pathogenic simian immunodeficiency virus infection. *J. Immunol.* 180: 5530–5536.
13. Tesselaar, K., R. Arens, G. M. van Schijndel, P. A. Baars, M. A. van der Valk, J. Borst, M. H. van Oers, and R. A. van Lier. 2003. Lethal T cell immunodeficiency induced by chronic costimulation via CD27-CD70 interactions. *Nat. Immunol.* 4: 49–54.
14. Baenziger, S., M. Heikenwalder, P. Johansen, E. Schlaepfer, U. Hofer, R. C. Miller, S. Diemand, K. Honda, T. M. Kundig, A. Aguzzi, and R. F. Speck. 2009. Triggering TLR7 in mice induces immune activation and lymphoid system disruption, resembling HIV-mediated pathology. *Blood* 113: 377–388.
15. Silvestri, G., M. Paiardini, I. Pandrea, M. M. Lederman, and D. L. Sodora. 2007. Understanding the benign nature of SIV infection in natural hosts. *J. Clin. Invest.* 117: 3148–3154.
16. Brenchley, J. M., D. A. Price, T. W. Schacker, T. E. Asher, G. Silvestri, S. Rao, Z. Kazzaz, E. Bornstein, O. Lambotte, D. Altmann, et al. 2006. Microbial translocation is a cause of systemic immune activation in chronic HIV infection. *Nat. Med.* 12: 1365–1371.
17. Appay, V., and D. Sauce. 2008. Immune activation and inflammation in HIV-1 infection: causes and consequences. *J. Pathol.* 214: 231–241.
18. Marchetti, G., C. Tincati, and G. Silvestri. 2013. Microbial translocation in the pathogenesis of HIV infection and AIDS. *Clin. Microbiol. Rev.* 26: 2–18.
19. Appay, V., and A. D. Kelleher. 2016. Immune activation and immune aging in HIV infection. *Curr. Opin. HIV AIDS* 11: 242–249.
20. Korn, T., E. Bettelli, M. Oukka, and V. K. Kuchroo. 2009. IL-17 and Th17 cells. *Annu. Rev. Immunol.* 27: 485–517.
21. Brenchley, J. M., M. Paiardini, K. S. Knox, A. I. Asher, B. Cervasi, T. E. Asher, P. Scheinberg, D. A. Price, C. A. Hage, L. M. Kholi, et al. 2008. Differential Th17 CD4 T-cell depletion in pathogenic and nonpathogenic lentiviral infections. *Blood* 112: 2826–2835.
22. Cecchinato, V., C. J. Trindade, A. Laurence, J. M. Heraud, J. M. Brenchley, M. G. Ferrari, L. Zaffiri, E. Tryniszewska, W. P. Tsai, M. Vaccari, et al. 2008. Altered balance between Th17 and Th1 cells at mucosal sites predicts AIDS progression in simian immunodeficiency virus-infected macaques. *Mucosal Immunol.* 1: 279–288.
23. Raffatellu, M., R. L. Santos, D. E. Verhoeven, M. D. George, R. P. Wilson, S. E. Winter, I. Godinez, S. Sankaran, T. A. Paixao, M. A. Gordon, et al. 2008. Simian immunodeficiency virus-induced mucosal interleukin-17 deficiency promotes *Salmonella* dissemination from the gut. *Nat. Med.* 14: 421–428.
24. Ciccone, E. J., J. H. Greenwald, P. I. Lee, A. Biancotto, S. W. Read, M. A. Yao, J. N. Hodge, W. L. Thompson, S. B. Kovacs, C. L. Chairez, et al. 2011. $CD4^+$ T cells, including Th17 and cycling subsets, are intact in the gut mucosa of HIV-1-infected long-term nonprogressors. *J. Virol.* 85: 5880–5888.
25. Salgado, M., N. I. Rallón, B. Rodés, M. López, V. Soriano, and J. M. Benito. 2011. Long-term non-progressors display a greater number of Th17 cells than HIV-infected typical progressors. *Clin. Immunol.* 139: 110–114.
26. Macal, M., S. Sankaran, T. W. Chun, E. Reay, J. Flamm, T. J. Prindiville, and S. Dandekar. 2008. Effective $CD4^+$ T-cell restoration in gut-associated lymphoid tissue of HIV-infected patients is associated with enhanced Th17 cells and polyfunctional HIV-specific T-cell responses. *Mucosal Immunol.* 1: 475–488.
27. d'Ettorre, G., S. Baroncelli, L. Micci, G. Ceccarelli, M. Andreotti, P. Sharma, G. Fanello, F. Fiocca, E. N. Cavallari, N. Giustini, et al. 2014. Reconstitution of intestinal CD4 and Th17 T cells in antiretroviral therapy suppressed HIV-infected subjects: implication for residual immune activation from the results of a clinical trial. *PLoS One* 9: e109791.
28. Chun, T. W., S. Moir, and A. S. Fauci. 2015. HIV reservoirs as obstacles and opportunities for an HIV cure. *Nat. Immunol.* 16: 584–589.
29. Gosselin, A., P. Monteiro, N. Chomont, F. Diaz-Griffero, E. A. Said, S. Fonseca, V. Wacleche, M. El-Far, M. R. Boulassel, J. P. Routy, et al. 2010. Peripheral blood $CCR4^+CCR6^+$ and $CXCR3^+CCR6^+CD4^+$ T cells are highly permissive to HIV-1 infection. *J. Immunol.* 184: 1604–1616.
30. El Hed, A., A. Khaitan, L. Kozhaya, N. Manel, D. Daskalakis, W. Borkowsky, F. Valentine, D. R. Littman, and D. Unutmaz. 2010. Susceptibility of human Th17 cells to human immunodeficiency virus and their perturbation during infection. *J. Infect. Dis.* 201: 843–854.
31. Monteiro, P., A. Gosselin, V. S. Wacleche, M. El-Far, E. A. Said, H. Kared, N. Grandvaux, M. R. Boulassel, J. P. Routy, and P. Ancuta. 2011. Memory $CCR6^+CD4^+$ T cells are preferential targets for productive HIV type 1 infection regardless of their expression of integrin β_7. *J. Immunol.* 186: 4618–4630.
32. Alvarez, Y., M. Tuen, G. Shen, F. Nawaz, J. Arthos, M. J. Wolff, M. A. Poles, and C. E. Hioe. 2013. Preferential HIV infection of $CCR6^+$ Th17 cells is associated with higher levels of virus receptor expression and lack of CCR5 ligands. *J. Virol.* 87: 10843–10854.
33. Wang, C., S. G. Kang, J. Lee, Z. Sun, and C. H. Kim. 2009. The roles of CCR6 in migration of Th17 cells and regulation of effector T-cell balance in the gut. *Mucosal Immunol.* 2: 173–183.
34. Acosta-Rodriguez, E. V., L. Rivino, J. Geginat, D. Jarrossay, M. Gattorno, A. Lanzavecchia, F. Sallusto, and G. Napolitani. 2007. Surface phenotype and antigenic specificity of human interleukin 17-producing T helper memory cells. *Nat. Immunol.* 8: 639–646.
35. Kader, M., X. Wang, M. Piatak, J. Lifson, M. Roederer, R. Veazey, and J. J. Mattapallil. 2009. $\alpha4^+\beta7^{hi}CD4^+$ memory T cells harbor most Th-17 cells and are preferentially infected during acute SIV infection. *Mucosal Immunol.* 2: 439–449.
36. Ryan, E. S., L. Micci, R. Fromentin, S. Paganini, C. S. McGary, K. Easley, N. Chomont, and M. Paiardini. 2016. Loss of function of intestinal IL-17 and IL-22 producing cells contributes to inflammation and viral persistence in SIV-infected rhesus macaques. *PLoS Pathog.* 12: e1005412.
37. Thelen, M., and J. V. Stein. 2008. How chemokines invite leukocytes to dance. *Nat. Immunol.* 9: 953–959.
38. Ghosh, M., X. Song, G. Mouneimne, M. Sidani, D. S. Lawrence, and J. S. Condeelis. 2004. Cofilin promotes actin polymerization and defines the direction of cell motility. *Science* 304: 743–746.
39. Arber, S., F. A. Barbayannis, H. Hanser, C. Schneider, C. A. Stanyon, O. Bernard, and P. Caroni. 1998. Regulation of actin dynamics through phosphorylation of cofilin by LIM-kinase. *Nature* 393: 805–809.
40. Yang, N., O. Higuchi, K. Ohashi, K. Nagata, A. Wada, K. Kangawa, E. Nishida, and K. Mizuno. 1998. Cofilin phosphorylation by LIM-kinase 1 and its role in Rac-mediated actin reorganization. *Nature* 393: 809–812.
41. Schultheiss, T., N. Stolte-Leeb, S. Sopper, and C. Stahl-Hennig. 2011. Flow cytometric characterization of the lymphocyte composition in a variety of mucosal tissues in healthy rhesus macaques. *J. Med. Primatol.* 40: 41–51.
42. Schoeni-Affolter, F., B. Ledergerber, M. Rickenbach, C. Rudin, H. F. Günthard, A. Telenti, H. Furrer, S. Yerly, and P. Francioli, Swiss HIV Cohort Study. 2010. Cohort profile: the swiss HIV cohort study. *Int. J. Epidemiol.* 39: 1179–1189.
43. Sallusto, F., and A. Lanzavecchia. 1994. Efficient presentation of soluble antigen by cultured human dendritic cells is maintained by granulocyte/macrophage colony-stimulating factor plus interleukin 4 and downregulated by tumor necrosis factor alpha. *J. Exp. Med.* 179: 1109–1118.
44. Schindelin, J., I. Arganda-Carreras, E. Frise, V. Kaynig, M. Longair, T. Pietzsch, S. Preibisch, C. Rueden, S. Saalfeld, B. Schmid, et al. 2012. Fiji: an open-source platform for biological-image analysis. *Nat. Methods* 9: 676–682.
45. Valentin, A., M. Rosati, D. J. Patenaude, A. Hatzakis, L. G. Kostrikis, M. Lazanas, K. M. Wyvill, R. Yarchoan, and G. N. Pavlakis. 2002. Persistent HIV-1 infection of natural killer cells in patients receiving highly active antiretroviral therapy. *Proc. Natl. Acad. Sci. USA* 99: 7015–7020.
46. Negri, D. R., S. Baroncelli, S. Catone, A. Comini, Z. Michelini, M. T. Maggiorella, L. Sernicola, F. Crostarosa, R. Belli, M. G. Mancini, et al. 2004. Protective efficacy of a multicomponent vector vaccine in cynomolgus monkeys after intrarectal simian immunodeficiency virus challenge. *J. Gen. Virol.* 85: 1191–1201.
47. Panzer, U., and M. Uguccioni. 2004. Prostaglandin E_2 modulates the functional responsiveness of human monocytes to chemokines. *Eur. J. Immunol.* 34: 3682–3689.
48. Yoder, A., D. Yu, L. Dong, S. R. Iyer, X. Xu, J. Kelly, J. Liu, W. Wang, P. J. Vorster, L. Agulto, et al. 2008. HIV envelope-CXCR4 signaling activates

cofilin to overcome cortical actin restriction in resting CD4 T cells. *Cell* 134: 782–792.
49. Stolp, B., and O. T. Fackler. 2011. How HIV takes advantage of the cytoskeleton in entry and replication. *Viruses* 3: 293–311.
50. Stolp, B., L. Abraham, J. M. Rudolph, and O. T. Fackler. 2010. Lentiviral Nef proteins utilize PAK2-mediated deregulation of cofilin as a general strategy to interfere with actin remodeling. *J. Virol.* 84: 3935–3948.
51. Vorster, P. J., J. Guo, A. Yoder, W. Wang, Y. Zheng, X. Xu, D. Yu, M. Spear, and Y. Wu. 2011. LIM kinase 1 modulates cortical actin and CXCR4 cycling and is activated by HIV-1 to initiate viral infection. *J. Biol. Chem.* 286: 12554–12564.
52. Lécureuil, C., B. Combadière, E. Mazoyer, O. Bonduelle, A. Samri, B. Autran, P. Debré, and C. Combadière. 2007. Trapping and apoptosis of novel subsets of memory T lymphocytes expressing CCR6 in the spleen of HIV-infected patients. *Blood* 109: 3649–3657.
53. Mavigner, M., M. Cazabat, M. Dubois, F. E. L'Faqihi, M. Requena, C. Pasquier, P. Klopp, J. Amar, L. Alric, K. Barange, et al. 2012. Altered $CD4^+$ T cell homing to the gut impairs mucosal immune reconstitution in treated HIV-infected individuals. *J. Clin. Invest.* 122: 62–69.
54. Reinhart, T. A., S. Qin, and Y. Sui. 2009. Multiple roles for chemokines in the pathogenesis of SIV infection. *Curr. HIV Res.* 7: 73–82.
55. Perez-Patrigeon, S., B. Vingert, O. Lambotte, J. P. Viard, J. F. Delfraissy, J. Thèze, and L. A. Chakrabarti. 2009. HIV infection impairs CCR7-dependent T-cell chemotaxis independent of CCR7 expression. *AIDS* 23: 1197–1207.
56. Stolp, B., A. Imle, F. M. Coelho, M. Hons, R. Gorina, R. Lyck, J. V. Stein, and O. T. Fackler. 2012. HIV-1 Nef interferes with T-lymphocyte circulation through confined environments in vivo. *Proc. Natl. Acad. Sci. USA* 109: 18541–18546.
57. Spear, M., J. Guo, A. Turner, D. Yu, W. Wang, B. Meltzer, S. He, X. Hu, H. Shang, J. Kuhn, and Y. Wu. 2014. HIV-1 triggers WAVE2 phosphorylation in primary CD4 T cells and macrophages, mediating Arp2/3-dependent nuclear migration. *J. Biol. Chem.* 289: 6949–6959.
58. Wu, Y., A. Yoder, D. Yu, W. Wang, J. Liu, T. Barrett, D. Wheeler, and K. Schlauch. 2008. Cofilin activation in peripheral CD4 T cells of HIV-1 infected patients: a pilot study. *Retrovirology* 5: 95.
59. Mandl, J. N., A. P. Barry, T. H. Vanderford, N. Kozyr, R. Chavan, S. Klucking, F. J. Barrat, R. L. Coffman, S. I. Staprans, and M. B. Feinberg. 2008. Divergent TLR7 and TLR9 signaling and type I interferon production distinguish pathogenic and nonpathogenic AIDS virus infections. *Nat. Med.* 14: 1077–1087.
60. He, X., H. Jia, Z. Jing, and D. Liu. 2013. Recognition of pathogen-associated nucleic acids by endosomal nucleic acid-sensing Toll-like receptors. *Acta Biochim. Biophys. Sin. (Shanghai)* 45: 241–258.
61. Mir, K. D., S. E. Bosinger, M. Gasper, O. Ho, J. G. Else, J. M. Brenchley, D. J. Kelvin, G. Silvestri, S. L. Hu, and D. L. Sodora. 2012. Simian immunodeficiency virus-induced alterations in monocyte production of tumor necrosis factor alpha contribute to reduced immune activation in sooty mangabeys. *J. Virol.* 86: 7605–7615.
62. Klatt, N. R., N. T. Funderburg, and J. M. Brenchley. 2013. Microbial translocation, immune activation, and HIV disease. *Trends Microbiol.* 21: 6–13.